1 **The type IVa pilus machinery is pre-installed during cell division**

2

3 Tyson Carter[1], Ryan N.C. Buensuceso[1], Stephanie Tammam[2], Ryan P. Lamers[1],

4 Hanjeong Harvey[1], P. Lynne Howell[2,3#], and Lori L. Burrows[1#].

5

6 [1]Department of Biochemistry and Biomedical Sciences and the Michael G. DeGroote

7 Institute for Infectious Disease Research, McMaster University, ON, CANADA;

8 [2]Program in Molecular Structure & Function, The Hospital for Sick Children; and

9 [3]Department of Biochemistry, University of Toronto, ON, CANADA.

10

11 **Running title**: Pre-installation of the type IV pilus machinery

12

13 **[#]To whom correspondence should be addressed:**

14 Dr. Lori L. Burrows, 4H18 Health Sciences Centre, 1200 Main St. West, Hamilton, ON,

15 L8N 3Z5 CANADA, Tel: (905)-525-9140 ext: 22029, Fax: (905) 522-9033, E-mail:

16 burrowl@mcmaster.ca

17 Dr. P. Lynne Howell, 20-9-715 Peter Giligan Centre for Research and Learning, 686 Bay

18 St., Toronto, ON M5G 0A4 CANADA, Tel: (416) 813-5378, Fax: (416) 813-5022, E-mail:

19 howell@sickkids.ca

20

21

22

23

24   **ABSTRACT**

25   Type IV pili (T4aP) are ubiquitous microbial appendages used for adherence, twitching

26   motility, DNA uptake, and electron transfer. Many of these functions depend on dynamic

27   assembly and disassembly of the pilus by a megadalton-sized, cell envelope-spanning

28   protein complex located at the poles of rod-shaped bacteria. How the T4aP assembly

29   complex becomes integrated into the cell envelope in the absence of dedicated

30   peptidoglycan (PG) hydrolases is unknown. After ruling out potential involvement of

31   housekeeping PG hydrolases in installation of the T4aP machinery in *P. aeruginosa*, we

32   discovered that key components of inner (PilMNOP) and outer (PilQ) membrane

33   subcomplexes are recruited to future sites of cell division. Mid-cell recruitment of a

34   fluorescently tagged alignment subcomplex component, mCherry-PilO, depended on

35   PilQ secretin monomers - specifically, their N-terminal PG-binding AMIN domains. PilP,

36   which connects PilO to PilQ, was required for recruitment, while PilM, which is

37   structurally similar to divisome component FtsA, was not. Recruitment preceded secretin

38   oligomerization in the outer membrane, as loss of the PilQ pilotin, PilF, had no effect on

39   localization. These results were confirmed in cells chemically blocked for cell division

40   prior to outer membrane invagination. The hub protein FimV and a component of the

41   Polar Organelle Coordinator complex - PocA - were independently required for mid-cell

42   recruitment of PilO and PilQ. Together, these data reveal an integrated, energy-efficient

43   strategy for the targeting and pre-installation – rather than retrofit - of the T4aP system

44   into nascent poles, without the need for dedicated PG-remodelling enzymes.

45

46

47 **IMPORTANCE**

48   The peptidoglycan (PG) layer of bacterial cell envelopes has limited porosity,

49 representing a physical barrier to insertion of large protein complexes involved in

50 secretion and motility. Many systems include dedicated PG hydrolase components that

51 create space for their insertion, but the ubiquitous type IVa pilus (T4aP) system lacks

52 such an enzyme. Instead, we found that components of the T4aP system are recruited

53 to future sites of cell division where they can be incorporated into the cell envelope

54 during the formation of new poles, eliminating the need for PG hydrolases. Targeting

55 depends on the presence of septal PG-binding motifs in specific components, as

56 removal of those motifs causes delocalization. This pre-installation strategy for the T4aP

57 assembly system ensures that both daughter cells are poised to extrude pili from new

58 poles as soon as they separate from one another.

59

60 **INTRODUCTION**

61   The cell envelopes of most gram-negative bacteria are comprised of an inner

62 membrane, a peptidoglycan (PG) layer found in the periplasm, and an outer membrane

63 (OM). A variety of large protein complexes, including motility machines, secretion

64 systems, and efflux pumps span all these layers (1), but in many cases the mechanisms

65 used to integrate these systems into the cell envelope remain uncharacterized. In many

66 cases, they are integrated at specific locations in the cell such as the poles, which is

67 important for their function.

68   The machinery that assembles and disassembles type IVa pili (T4aP) is among

69 the most common cell envelope-spanning complexes found in gram-negative bacteria.

70   T4aP are long, thin protein fibres used for adherence, biofilm formation and a flagellum-

71   independent form of motility known as twitching, defined as repeated cycles of pilus

72   extension, adherence to a surface, and retraction of the pilus fibre (2, 3). *P. aeruginosa*

73   T4aP are important for surface mechanosensing and consequent up-regulation of

74   virulence factor expression (4), and for the delivery of toxins by other secretion systems

75   (5, 6). In the absence of T4aP, *P. aeruginosa* has reduced pathogenicity (5).

76   The T4aP machinery is composed of four subcomplexes that together form a

77   dynamic cylindrical machine (3, 7, 8). The inner membrane motor and alignment

78   subcomplexes form the platform for assembly and disassembly of the pilus, and interact

79   directly with the secretin that allows for pilus extrusion through the OM. The OM

80   lipoprotein PilF promotes formation of the secretin, a highly stable oligomer of 14 PilQ

81   subunits that form a gated channel in the OM (9, 10). The N-terminus of each PilQ

82   monomer contains two tandem amidase N-terminal (AMIN) domains, involved in binding

83   peptidoglycan (11-13). The alignment subcomplex composed of PilMNOP connects the

84   motor subcomplex with the secretin, and participates in pilus extension and retraction

85   (14-17). PilM is a cytoplasmic, actin-like protein that clamps tightly onto the short amino-

86   terminus of the inner membrane protein, PilN, which in turn forms heterodimers with

87   inner membrane protein, PilO (14, 18, 19). The inner membrane lipoprotein PilP

88   interacts with PilNO heterodimers via its long unstructured N-terminus, and with the

89   periplasmic N0 domain of PilQ via its C-terminal homology region (HR) domain,

90   completing the transenvelope complex (17, 20).

91   T4aP are usually located at the poles of rod-shaped cells, which promotes

92   adherence by minimizing surface area and thus electrostatic repulsion (3). How the

4

93   multi-protein T4aP system is initially targeted to and integrated into the poles of *P.*

94   *aeruginosa* cells are not well understood. Type III (T3SS) and Type IV (T4SS) secretion

95   systems have dedicated PG-remodelling enzymes that allow for retrofitting of the

96   complexes into the cell envelope (1). There are no such enzymes associated with the

97   T4aP system, suggesting that it uses an alternate pathway for cell envelope integration.

98   Here we used fluorescent fusions to an informative alignment subcomplex component,

99   PilO, and to the secretin monomer, PilQ, to track and quantify their localization in *P.*

100   *aeruginosa* wild type and mutant backgrounds. The results show that PilO and

101   associated components are recruited to future sites of cell division by the concerted

102   action of least three pathways. We propose that the T4aP machinery is preinstalled

103   during formation of nascent cell poles, a strategy that eliminates the need for dedicated

104   cell-wall-processing enzymes.

105

106   **RESULTS**

107   **mCherry-PilO localizes to cell poles and future cell division sites**

108   When selecting components of the T4aP machinery to track using fluorescent

109   fusions, we considered the known interactions and stoichiometry of these proteins and

110   how a fusion might affect function. PilM is cytoplasmic, but has multiple interaction

111   partners (14, 19, 20), including PilN, whose cytoplasmic N-terminus binds to a groove on

112   PilM; thus, we excluded both as candidates. PilN interacts along most of its remaining

113   length with PilO (15, 21), but PilO's cytoplasmic N-terminus is poorly conserved among

114   T4aP-expressing species (16), supporting the observation that it appears to have no

115   cytoplasmic interaction partners. Therefore, PilO was selected as a fusion candidate for

5

116   localization of the alignment subcomplex. To maintain the physiological expression

117   levels and stoichiometry that are important for function (14), a *pilO* construct encoding

118   an in-frame fusion of mCherry to the N-terminus of PilO was used to replace the WT

119   version at the native *pilO* locus (**Fig. 1A**). Stability and functionality of the fusion protein

120   were verified by western blot with anti-PilO and anti-mCherry antisera, and assessment

121   of twitching motility, respectively (**Fig. 1B**).

122   mCherry-PilO localized to both poles, as well as to the midpoint of cells

123   undergoing division (**Fig. 1C**). To more clearly visualize the predivisional localization

124   pattern of mCherry-PilO, cells were treated with sub-inhibitory levels of cefsulodin, which

125   inhibits PBP3 (FtsI), a late-stage PG transpeptidase, leading to division arrest and

126   filamentation (22). In filamented cells, mCherry-PilO localized to the poles and to

127   regularly spaced foci, suggestive of recruitment to future sites of cell division (**Fig. 1D**).

128   Quantification of mCherry-PilO localization in wild type cells (**Fig. 1E**) confirmed its

129   predominately bipolar localization.

130   To provide further evidence that mCherry-PilO was recruited to sites of cell

131   division, the *minC* gene, which encodes a key component of the oscillating Min system

132   required for inhibition of FtsZ polymerization at non-mid-cell locations (23, 24) was

133   deleted in the mCherry-PilO strain. Cells lacking MinC exhibit aberrantly localized septa,

134   producing mini-cells due to unequal cell division (**Fig. 2A**). As predicted, the mCherry-

135   PilO fusion continued to localize to polar and septal sites despite their aberrant

136   placement (**Fig. 2B**). Together, these data suggest that when expressed under

137   physiological conditions, PilO – and by inference, its interaction partners, PilMN and PilP

138   (20) – are recruited to future sites of cell division.

139

140 **PilQ monomers are required for T4aP alignment subcomplex localization**

141   To define the mechanism of recruitment of the T4aP alignment subcomplex to

142 sites of cell division, we first examined the effects of deleting specific subcomplex

143 components. The cytoplasmic member of the alignment subcomplex, PilM, has

144 pronounced structural similarity ($C\alpha$ root mean square deviation = 1.9 Å over 257

145 residues) to the early divisome protein, FtsA, a peripheral inner membrane protein

146 whose interaction with FtsZ tethers the latter to the membrane (18, 19). Based on its

147 structural mimicry of FtsA and its peripheral membrane localization via binding of PilN's

148 amino terminus, we previously hypothesized (25) that PilM – and thus the alignment

149 subcomplex – might be recruited to mid-cell through interactions with the FtsZ ring.

150 However, mCherry-PilO exhibited polar and mid-cell localization in a *pilM* mutant (**Fig.**

151 **3AB**), ruling out PilM as a driver of recruitment.

152   The PilMNOP alignment subcomplex connects to the secretin via interaction of

153 the C-terminal HR domain of PilP with the periplasmic N0 domain of PilQ (20).

154 Preceding the N0 domain in *P. aeruginosa* PilQ are two tandem AMIN domains,

155 predicted to bind septal PG (11-13). To test their PG-binding ability, we cloned,

156 expressed, and purified 3 fragments of PilQ's N-terminal region (the AMIN domains

157 alone; the N0-N1 domains alone; and all 4 domains together), and performed pulldown

158 assays using purified *P. aeruginosa* PG (**Supplementary Fig. S1**). In the absence of

159 PG, all fragments remained in the soluble fraction; however, when insoluble PG was

160 present, only those fragments containing the AMIN domains were also found in the

161 insoluble fraction, indicating that they bind PG.

162   Since *pilMNOPQ* are expressed from a single operon, we hypothesized that

163   recruitment of PilMNOP to sites of cell division might occur through a series of PilMNOP-

164   PilQ-septal PG interactions. We first confirmed that PilQ-mCherry was localized to the

165   poles and to regularly spaced foci in filamented cells, a pattern similar to mCherry-PilO

166   (**Supplementary Fig. S2**). When we deleted *pilQ*, mCherry-PilO became delocalized

167   (**Fig. 3CD**). To confirm that loss of mCherry-PilO localization in the *pilQ* strain was

168   indirectly due to loss of PilP-PilQ interactions, *pilP* was deleted in the mCherry-PilO

169   strain. In the *pilP* mutant, mCherry-PilO was delocalized (**Fig. 3EF**), supporting the

170   hypothesis that recruitment of PilQ to mid-cell is the primary event, and the remaining

171   alignment subcomplex components are recruited via their interaction with PilP, and its

172   interaction with PilQ.

173   To test whether its AMIN domains were responsible for localization of PilQ and its

174   interaction partners to mid-cell and polar positions, we complemented a *pilQ* mutant

175   expressing mCherry-PilO with full length *pilQ*, or a construct expressing only the N0-N1

176   and secretin domains, previously shown to form stable but non-functional secretin

177   oligomers (**Fig. 4A**) (9). Full length PilQ restored the wild type pattern of mCherry-PilO

178   localization (**Fig. 4BC**), but the AMIN-deficient PilQ did not (**Fig. 4DE**). These data show

179   that localization of T4aP assembly components is dependent upon PilQ's AMIN

180   domains, which interact with PG (**Supplementary Fig. S1**).

181

182   **Localization of mCherry-PilO precedes PilQ oligomerization**

183   The *Myxococcus xanthus* T4aP system was proposed to assemble in an 'outside-

184   in' manner, with PilMNOP alignment subcomplexes docking onto the PilQ secretin after

8

185   its assembly in the OM (26). Those data are not consistent with our observation that

186   mCherry-PilO localized to regularly spaced foci in chemically-filamented *P. aeruginosa*

187   cells (**Fig. 1**), where the OM is not yet invaginated due to arrest of cell division. To test

188   whether secretin oligomerization was a necessary prerequisite for recruitment, we

189   examined localization of PilQ-mCherry in mutants lacking the OM lipoprotein PilF. In the

190   absence of PilF, PilQ remains in a monomeric state in the inner membrane (9), but its

191   localization pattern was unchanged compared to wild type (**Supplementary Fig. S2AB**).

192   Similarly, localization of mCherry-PilO in the *pilF* background resembled wild type (**Fig.**

193   **5**). These data confirm that localization of T4aP components to mid-cell – while PilQ-

194   dependent – precedes secretin oligomerization.

195

Additional factors modulate T4aP assembly machinery localization

197   FimV is a T4aP-associated protein required for twitching motility and has a highly

198   conserved PG-binding LysM motif in its periplasmic N-terminal domain (27, 28). We

199   showed previously (28) that PilQ multimer formation is reduced in a *fimV* mutant, which

200   made FimV of interest for this study. In the absence of FimV, mCherry-PilO was

201   delocalized (**Fig. 6AB**), as was PilQ-mCherry (**Supplementary Fig. S2C**). We

202   previously generated a strain expressing a variant of FimV with an in-frame deletion of

203   its LysM motif (28). mCherry-PilO (**Fig. 6CD**) was delocalized in the *fimV*$_{\Delta LysM}$ strain, as

204   was the majority of PilQ-mCherry (**Supplementary Fig. S2D**). These data suggest that

205   interactions of both PilQ and FimV with PG are important steps in the localization

206   process, and that polar localization of PilQ depends in part on FimV.

9

207   During a mutant screen looking for factors required for correct localization of *P.*

208   *aeruginosa*'s single polar flagellum, Cowles and colleagues (29) identified a putative

209   protein complex that they named PocAB -TonB3 for 'polar organelle coordinator'. Loss

210   of TonB3 had previously been shown to affect twitching motility (30), but the mechanism

211   was unknown. All three components were required for expression and/or polar

212   localization of T4aP. *pocA* mutants made a few, non-polar pili, while *pocB* and *tonB3*

213   mutants failed to produce pili. The mechanism by which this system controls polar

214   localization of motility organelles remains unclear, since the Poc proteins themselves

215   are not localized to the poles (29).

216   We focused on *pocA* as the mutant's ability to make a few pili suggested that the

217   T4aP assembly system was functional, and deleted it from cells expressing either

218   mCherry-PilO (**Fig. 7AB**) or PilQ-mCherry (**Supplementary Fig. S2E**). mCherry-PilO

219   was delocalized in the absence of *pocA*, and its wild type localization was re-established

220   upon complementation with *pocA in trans* (**Fig. 7CD**). PilQ-mCherry was delocalized in

221   the *pocA* background although some polar fluorescence remained (**Supplementary Fig.**

222   **S2E**). Interestingly, while both PocA and FimV were required for T4P assembly

223   component localization to polar and midcell locations, they appear to act independently

224   of one another. The fluorescent FimV fusion, which exhibits bipolar localization in wild

225   type cells, remained localized to the poles of a *pocA* mutant (**Fig. 8**).

226

227   **DISCUSSION**

228   The T4aP machinery spans all layers of the gram-negative cell envelope at the

229   poles of rod-shaped cells, but how this megadalton protein complex is installed in the

10

230   absence of dedicated PG hydrolyzing enzymes was unclear. Here we showed that

231   degradation of PG is unnecessary, because components of the *P. aeruginosa* T4P

232   alignment subcomplex and the secretin are recruited to sites of cell division where they

233   can be pre-installed, rather than retrofitted, into nascent poles. These data are

234   consistent with our observation that mutants lacking multiple housekeeping PG

235   hydrolases – which could potentially provide PG lytic activities for retrofitting in the

236   absence of system-specific enzymes – have correctly inserted, functional T4aP

237   machines, as demonstrated by their ability to twitch (**Supplementary Fig. S3**). Instead,

238   at least 3 different mechanisms participate in the process of T4aP polar localization in *P.*

239   *aeruginosa*, two of which (PilQ and FimV) depend on recognition of PG, as deletion of

240   PilQ's AMIN domains or FimV's LysM motif results in delocalization.

241   Cell poles are characterized by PG that has fewer stem peptides compared to

242   lateral wall PG, due to the activity of *N*-acetylmuramyl-L-alanine amidases that cleave

243   the amide bond between *N*-acetylmuramic acid and the stem peptides during daughter

244   cell separation (31-33). This denuded form of PG is the binding target for multiple

245   protein motifs, among them AMIN, SPOR, and LysM (28, 34-36). *P. aeruginosa* and *M.*

246   *xanthus* PilQ monomers have N-terminal AMIN domains (2 per monomer in *P.*

247   *aeruginosa* and 3 in *M. xanthus*), which in addition to targeting (37), may anchor secretin

248   complexes to the PG layer to counter the substantial forces generated during twitching

249   motility. *Neisseria gonorrhoeae* and *N. meningitidis* PilQ monomers also contain 2 AMIN

250   domains at their amino termini (11), yet they express peritrichous T4aP. *Neisseria* spp.

251   lack the cytoskeletal element MreB which patterns elongation of rod-shaped bacteria

252   (38), thus have a coccoid morphology. It's possible that the mechanism of T4aP

11

253   assembly system recruitment to sites of cell division is similar in *Neisseria* spp., but due

254   to their shape – the equivalent of two closely apposed poles – they appear to have

255   peritrichous T4aP distribution.

256   In the *P. aeruginosa* T4aP system, at least two different PG-binding proteins were

257   needed for correct positioning. We showed previously (28) that FimV binds PG via its

258   LysM motif, important for optimal secretin assembly. A number of recent studies showed

259   that FimV and related HubP proteins – which contain multiple protein-protein interaction

260   domains in addition to conserved LysM motifs – act as landmarks, responsible for polar

261   localization of other proteins, including those involved in regulation of T4aP function,

262   flagellar placement, and chromosome segregation (39-43). For example, *P. aeruginosa*

263   FimL – a regulatory protein important for T4aP assembly via its regulation of intracellular

264   cAMP levels – interacts with the C-terminal TPR motif of FimV (39, 44). Loss of FimV

265   also results in mislocalization of the core T4aP machinery (**Fig. 6**); thus FimV appears to

266   have both physical and regulatory roles in T4aP assembly and function.

267   Cowles *et al.* (29) reported that both the flagellum and T4aP were mislocalized in

268   *P. aeruginosa* mutants lacking the polar organelle coordinating (Poc) proteins, but the

269   mechanism remains enigmatic. The T4aP alignment subcomplex was delocalized in a

270   *pocA* mutant (**Fig. 7**) while FimV remained bipolar (**Fig. 8**), implying that they act

271   independently of one another – with the caveat that the FimV fusion used here was non-

272   functional in twitching motility. PocAB-TonB3 are homologous to the ExbBD-TonB

273   complex in *E. coli* (29) which energizes siderophore uptake across the OM via direct

274   interactions with the 'Ton box' on one beta strand of TonB-dependent receptors. The N0

275   domains of secretin monomers are structurally similar (2.3 Å root mean square deviation

12

276   over 65 residues) to the signalling domain of FpvA, a TonB-dependent siderophore

277   receptor in *P. aeruginosa* (45). This similarity hints at potential interactions between the

278   TonB3 component of the Poc complex and the N0 domain of PilQ monomers. We noted

279   that although deletion of *pocA* had no significant effect on cell morphology,

280   complementation with a plasmid-borne copy of the gene increased average cell length

281   by ~50% (**Supplementary Fig. S4**), suggesting that the Poc system might influence the

282   timing of cell division or affect PG remodelling. Subtle structural differences in PG

283   architecture in the absence of PocA could impact binding of proteins with PG targeting

284   motifs.

285   Mid-cell recruitment of mCherry-PilO was dependent on the secretin monomer

286   PilQ (**Fig. 3CD**) but deletion of the pilotin PilF had no effect (**Fig. 5**), showing that

287   recruitment and confinement of PilMNOPQ to cell division sites occur prior to secretin

288   oligomerization. Prior studies of *M. xanthus* T4aP assembly system formation suggested

289   that PilQ multimerization was essential for the recruitment of additional T4aP assembly

290   components, because loss of Tgl – the *M. xanthus* PilF homolog – abrogated polar

291   localization of PilQ and other T4aP proteins. These data supported an 'outside in' model

292   for *M. xanthus* T4aP system formation, dependent on PilQ oligomerization (26).

293   Interestingly, *M. xanthus* PilQ was suggested in that study to localize to the septum

294   either "late during cell division, or immediately after". These data are consistent with the

295   pattern of PilQ localization in *P. aeruginosa*: however, the pilotin proteins in *M. xanthus*

296   and *P. aeruginosa* appear to play somewhat different roles.

297   Together, the data led us to propose a pathway for T4aP assembly machinery

298   integration into the *P. aeruginosa* cell envelope in the absence of dedicated PG

299   hydrolases. We suggest that PilMNOPQ are co-translated, forming an IM-bound

300   subcomplex that diffuses laterally until the AMIN domains of PilQ monomers bind to

301   septal PG. FimV, which has the capacity to interact with septal PG via its Lys motif, may

302   also interact with components of the subcomplex to retain them at cell division sites. The

303   next steps are still unclear, as the oligomerization pathway for PilQ in the OM remains

304   unknown. We previously proposed (9) that co-translocation of the lipoprotein PilF and

305   PilQ monomers by the Lol system might promote PilQ insertion into the OM, where it

306   oligomerizes. In this new model, we suggest that PilF is translocated independently by

307   the Lol system to the OM, where it then scans for, binds to, and promotes translocation

308   of PilQ monomers from the inner to the OM during invagination in the final stages of cell

309   division.

310   Two lines of evidence support this new hypothesis. First, in *M. xanthus*, co-

311   incubation of *pilQ* and *tgl* (*pilF*) mutants, neither of which are able to twitch, allowed for

312   intercellular transfer of Tgl from the *pilQ* mutant to the *tgl* mutant and oligomerization of

313   the latter's PilQ monomers, restoring piliation and motility (46). Thus, Tgl already

314   present in the OM of the *pilQ* mutant could promote insertion and oligomerization of PilQ

315   monomers in the *tgl* mutant. Second, the ability of OM lipoproteins to interact with inner

316   membrane proteins across the periplasm is now well established, as exemplified by the

317   *E. coli* OM lipoproteins, LpoA and LpoB (47, 48). These proteins are essential for

318   stimulating the activities of the inner membrane PG synthases PBP1a and PBP1b,

319   respectively, through direct interactions with regulatory domains of those enzymes.

320   Once PilQ monomers reach the OM with the assistance of PilF, they may first form

321   conformational intermediates prior to maturation into stable, SDS-resistant oligomers. In

14

322   *N. gonorrhoeae,* certain point mutations in the secretin domain were associated with

323   formation of immature, leaky oligomers, rendering the cells more susceptible to beta

324   lactam antibiotics (49).

325   The above scenario for PilQ translocation suggests that the ~ 2 nm porosity of

326   PG (50) would not pose a physical barrier to secretin assembly, as individual monomers

327   (~77 kDa) are small enough to pass through its natural gaps. Retention of PilQ AMIN

328   interactions with septal PG during translocation and insertion of the C-terminal secretin

329   domain in the OM would ultimately place the AMIN domains 'under' the PG layer, where

330   they would be ideally positioned to counteract retraction forces imposed during twitching

331   motility. Because polar PG is less likely to be remodelled due to its limited side chain

332   content, the secretin would remain stably fixed to the cell wall. Studies of the half-life of

333   a single bacterial cell pole show that it can be hundreds of generations old (51); thus, it

334   is perhaps not surprising that secretin complexes are highly resistant to denaturation,

335   allowing them to last as long as the poles in which they are embedded.

336   Among the questions remaining is whether the interaction interface between PilP

337   and PilQ is altered during translocation of PilQ monomers to the OM. We established

338   that mid-cell localization of mCherry-PilO depends on PilP (**Fig. 3EF**), which interacts

339   with the N0 domain of PilQ monomers via its C-terminal HR domain (11, 20). PilP also

340   interacts with PilNO heterodimers via its long unstructured N-terminus (17). This flexible

341   tether might allow the C-terminal domain of PilP to remain connected to the N0 domain

342   of PilQ as secretin monomers transit from the inner to OM. Alternatively, PilP may be

343   repositioned relative to PilQ when the latter translocates to the OM. In the evolutionarily

344   related T2SS, multiple interaction interfaces between the HR domain of GspC (PilP) and

15

345   N0 of GspD (PilQ) have been identified through a combination of structural, biochemical,

346   and functional studies (45, 52, 53). These various interfaces – some of which are

347   mutually exclusive – were attributed to differences in experimental setup, but could also

348   reflect capture of different interaction states pre- and post-secretin oligomerization.

349   Studies to address these possibilities are currently underway.

350

351   **MATERIALS & METHODS**

352   **Strains, media and growth conditions**

353   Bacterial strains, plasmids, and primers used in this study are listed in Tables 1

354   and 2. *Escherichia coli* and *P. aeruginosa* were grown at 37°C in LB Lennox broth or on

355   LB 1.5% agar plates supplemented with antibiotics. The antibiotics and their respective

356   concentrations were: ampicillin (Ap), 100 µg/mL; carbenicillin (Cb), 200 µg/mL;

357   gentamicin (Gm), 15 µg/mL for *E. coli* strain and 30 µg/mL for *P. aeruginosa* strains,

358   unless otherwise stated. Plasmids were transformed by heat shock into chemically

359   competent *E. coli* cells or by electroporation into *P. aeruginosa* suspended in sterile

360   water. All constructs were verified by DNA sequencing (MOBIX Lab, McMaster

361   University).

362

363   **Generation of *P. aeruginosa* mutants**

364   Mutants were made using previously described methods (54). Deletion constructs

365   for generation of *minC* and *pilF* mutants were designed to include 500 nucleotides up

366   and downstream of the gene to be deleted, as well as the first and last 50 nucleotides of

367   the gene. Constructs were synthesized and cloned into pUC57 (Genscript, Piscataway,

368 NJ). Deletion inserts in pUC57 were subcloned into the pEX18Gm suicide vector (55)

369 using the 5' BamHI and the 3' HindIII restriction sites, and verified by DNA sequencing.

370 After verification, suicide vectors containing the mutant genes (*pilF* or *minC*) were

371 transformed into *E. coli* SM10 cells. Plasmids were then transferred by conjugation in a

372 1:9 ratio of *P. aeruginosa* to *E. coli*. The mixed culture was pelleted for 1 min at 2292 x

373 *g*, and the pellet was resuspended in a 100 µL aliquot of LB, spot-plated on LB agar,

374 and incubated overnight at 37 °C. The mating mixture was removed from the LB agar

375 using a sterile toothpick, resuspended in 1 mL of LB and the *E. coli* SM10 donor was

376 counterselected by plating the mixture on *Pseudomonas* isolation agar (PIA; Difco)

377 containing Gm (100 µg/ml). Gm-resistant *P. aeruginosa* colonies were streaked on LB

378 no salt plates containing sucrose (1% (w/v) bacto-tryptone, 5% (w/v) sucrose, 1.5%

379 agar, 0.5% (w/v) bacto-yeast extract) and incubated for 16 h at 30 °C. Select colonies

380 were then subcultured on LB agar and LB agar plus Gm, and Gm-sensitive colonies

381 were screened by PCR using appropriate primers (Table 2) to confirm integration.

382 Amplicons from colonies with the desired PCR profile were sequenced to confirm

383 incorporation of the mutation, and the *pilF* mutant was analyzed by western blot analysis

384 using an α-PilF antibody to verify loss of the gene product.

385 A *pilQ* KO construct containing an FRT-flanked Gm cassette was designed

386 previously (9). This construct was integrated into the PAK chromosome using a Flp-FRT

387 recombination system (55) and selected for using the methods described above with the

388 following modifications: following growth on sucrose, colonies were cultured on LB agar,

389 LB agar with Gm and LB agar plus Cb. Colonies that had undergone double

390 recombination, integrating *pilQ*::GmFRT into the chromosome without pEX18Ap (Cb

17

391   sensitive colonies), were selected. The Gm cassette was removed by Flp recombinase-

392   catalyzed excision, by conjugally transferring the Flp-expressing pFLP2 from SM10 cells

393   into PAK cells carrying the GmFRT-disrupted *pilQ* gene. SM10 cells were

394   counterselected on PIA containing Cb (200 µg/ml). pFLP2 was removed from *P.*

395   *aeruginosa* by streaking Cb-resistant colonies on LB agar, no salt, containing 5% (w/v)

396   sucrose for 16 h at 30 °C. Colonies were then cultured on LB agar and LB-agar

397   containing Gm or Cb. Cb and Gm sensitive colonies were screened by PCR using the

398   PilQ FRT-Chk primers listed in Table 2 to confirm the retention of the FRT scar. The *pilQ*

399   gene of mutant strains were sequenced to confirm correct incorporation of the mutation,

400   and analyzed by western blot with α-PilQ sera to confirm loss of the gene product.

401   The *pocA* deletion construct was created previously in the pEX18Tc suicide

402   vector (29). The *pocA* deletion insert was subcloned into pEX18Gm using EcoRI and

403   XbaI, and constructs verified by DNA sequencing. After verification, the suicide vector

404   containing the *pocA* deletion construct transformed into *E. coli* SM10 cells and the

405   mutation introduced into *P. aeruginosa* as described above.

406

Generation of a chromosomally encoded mCherry-PilO fusion

408   A construct encoding an fusion of mCherry (56) to the N-terminus of PilO, plus

409   700 nucleotides upstream of *pilO* and 700 nucleotides downstream of *pilO,* was

410   synthesized and cloned into pUC57 (Genscript, Piscataway, NJ). The mCherry-PilO-

411   encoding insert was subcloned into the suicide vector pEX18Gm using the 5' EcoRI and

412   the 3' HindIII restriction sites, constructs verified by DNA sequencing, and introduced

413   into chemically competent *E. coli* SM10 by heat shock. The plasmid was then

18

414   transferred by conjugation in a 1:9 ratio of *P. aeruginosa* (wild type or various T4aP

415   mutants) to *E. coli* as described above. Following counter selection and curing of

416   merodiploids by sucrose selection, integration of the mCherry-PilO fusion in Gm-

417   sensitive colonies was confirmed by PCR and DNA sequencing (Table 2). mCherry-PilO

418   expressing strains were analyzed using western blot analysis and twitching assays to

419   verify expression of an intact fluorescent fusion protein and – in the wild type – function

420   of the T4aP machinery, respectively.

421

422   **Generation of complementation constructs**

423   The *pilQ, pocA* and *pilF* genes were amplified by PCR using PAK chromosomal

424   DNA as the template (Table 2) and cloned into pBADGr (Table 1). The digested DNA

425   was purified and ligated into pBADGr with T4 DNA ligase, according to the

426   manufacturer's instructions. Ligation mixtures were then transformed into *E. coli* DH5α

427   cells and grown overnight at 37 °C on LB agar supplemented with the appropriate

428   antibiotics.

429   A construct encoding a truncated version of PilQ lacking its AMIN domains was

430   previously generated in the PAO1 strain (9). The same boundaries were used here to

431   generate a truncated version of PAK PilQ. The PilQ Clone Fwd and PilQ 5' Rev primers

432   were used to amplify the 5' end of the gene, excluding the first AMIN domain, and the

433   PilQ N0 Fwd and PilQ Clone Rev primers (Table 2) were used to amplify the remainder

434   of the gene beginning at the N0 domain and excluding the second AMIN domain.

435   Purified amplicons were digested with XbaI and ligated into pBADGr with T4 DNA

436   Ligase. The ligation product and pBADGr were then digested with EcoRI and HindIII and

19

437   ligated following the same protocol. The fidelity of the pBADGr-*pilQ* construct was

438   confirmed by sequencing using the pBADGr mcs Fwd and Rev primers (Table 2).

439   Since PilQ has a cleavable N-terminal signal sequence, and a C-terminus that is

440   exposed to the extracellular environment (9, 57), we designed a construct encoding an

441   internal fusion of mCherry to PilQ (between the first and second AMIN domains,

442   residues 132 and 133), which was synthesized and subcloned into pUC57 (Genscript).

443   The PilQ-mCherry-encoding insert was subcloned into the complementation vector

444   pBADGr (58) using the 5' EcoRI and the 3' HindIII restriction sites and verified by DNA

445   sequencing. The construct was then introduced into PAK *pilQ*::FRT cells by

446   electroporation. Expression of the PilQ-mCherry fusion was verified using western blot

447   analysis with α-PilQ and α-mCherry antibodies and function was verified using twitching

448   assays (59).

449   The *yfp* gene encoding Yellow Fluorescent Protein (YFP) was cloned into the

450   HindIII restriction site of pBADGr. Correct insertion of the pBADGr-*yfp* construct was

451   confirmed by DNA sequencing using mcs Fwd/Rev primers (Table 2). A version of *fimV*

452   lacking its stop codon was amplified using the FimV Clone Fwd/Rev primers (Table 2)

453   and cloned into pBADGr in frame with the *yfp* gene by digesting both the vector and

454   insert with KpnI and XbaI restriction enzymes and ligating with T4 DNA ligase.

455   Successful ligation of the insert was confirmed using the pBADGr multiple cloning site

456   flanking primers (Table 2) and DNA sequencing. The construct was then electroporated

457   into *ΔfimV* and *ΔpocA* cells. A stable fusion of YFP to the C-terminus of FimV was

458   confirmed by western blotting with α-AFP and α-FimV antibodies. This fusion is

459   considered non-functional as it failed to restore twitching in the *fimV* background.

20

460   **Twitching motility assays**

461   Twitching motility assays were performed as previously described (59). Single

462   colonies were stab inoculated to the bottom of a 1% LB agar plate. Plates were

463   incubated for 24 h at 30 °C. Following incubation, the agar was removed and the

464   adherent bacteria stained with 1% (w/v) crystal violet for 30 min, followed by washing

465   with water to remove unbound dye. Twitching zones were photographed and their areas

466   measured using Fiji (60). All experiments were performed in triplicate with at least three

467   independent replicates.

468

469   **Analysis of whole cell lysates by western blot**

470   Cultures were grown overnight at 37 °C in LB supplemented with appropriate

471   antibiotics and diluted to an OD_{600} of 0.6. A 1 mL aliquot of cells was collected by

472   centrifugation at 2292 x *g* for 1 min. and the cell pellet was resuspended in 100 µl of

473   SDS sample buffer (80 mM Tris (pH 6.8), 5.3% (v/v) 2- mercaptoethanol, 10% (v/v)

474   glycerol, and 0.02% (w/v) bromophenol blue, and 2% (w/v) SDS) and boiled for 10 min.

475   Equal volumes of whole cell lysates were separated by 12.5% SDS-PAGE at 80-

476   150 V and transferred to nitrocellulose membranes for 1 h at 225 mA. Membranes were

477   blocked using 5% (w/v) low fat skim milk powder in phosphate buffered saline solution

478   (PBS) at pH 7.4 for 1 h at room temperature, followed by incubation with the appropriate

479   polyclonal (for PilF, PilM, PilO, PilP, PilQ, FimV) or monoclonal (for mCherry) antisera

480   for 1 h at room temperature. Membranes were washed twice in 10 mL of PBS for 5 min

481   then incubated in either goat-anti-rabbit or goat-anti-mouse IgG-alkaline phosphatase

482   conjugated secondary antibody (Bio-Rad) at a dilution of 1:3000 for 1 h at room

21

483   temperature. Membranes were washed twice in PBS for 5 min, and developed in a

484   solution containing 100 μL nitro-blue tetrazolium (NBT) and 100 μL 5-bromo-4-chloro-3-

485   indolyl phosphate (BCIP) in 10 mL of alkaline phosphatase buffer (100 mM NaCl, 5 mM

486    $MgCl_2$, 100 mM Tris, pH 9.5).

487

488   **Cell preparation for transmission electron microscopy**

489   Cells from a 1 mL overnight culture in LB were pelleted at 2292 x *g* and

490   resuspended in a 1 mL solution of 2% (w/v) gluteraldehyde in 0.1M sodium cacodylate

491   buffer at a pH of 7.4. Cells were fixed in solution for 2 h at 4 °C, and washed twice with

492   cold sodium cacodylate buffer (pH 7.4). Samples were then treated with 1% osmium

493   tetroxide in 0.1M sodium cacodylate for 1 h and stained with 2% uranyl acetate

494   overnight. After staining, cells were dehydrated gradually with ethanol, treated with

495   propylene oxide, embedded in Spurr's resin, and polymerized at 60 °C overnight. The

496   polymerized samples were sectioned using a Leica UCT ultramicrotome and post-

497   stained with 2% uranyl acetate and lead citrate. The prepared specimens were

498   examined in McMaster University's Electron Microscopy Facility using the JEOL JEM

499   1200 EX TEMSCAN microscope (JEOL, Peabody, MA, USA) operating at an

500   accelerating voltage of 80kV. Images were acquired with an AMT 4-megapixel digital

501   camera (Advanced Microscopy Techniques, Woburn, MA).

502

503   **Fluorescence Microscopy**

504   Strains were incubated overnight at 37 °C in 5 mL of LB supplemented with the

505   appropriate antibiotics. One mL of cells were pelleted at 2292 x *g*, and resuspended in 1

22

506   mL of sterile water containing 10 µg/ml of either Fm1-43 Fx (for cells expressing

507   mCherry) or Fm1-64 Fx (for cells expressing YFP) membrane stain (Invitrogen). Cells

508   were mixed with dye by gentle pipetting, and pelleted at 2292 x *g*. Pelleted cells were

509   then stab-inoculated using a pipette tip to the coverslip-media interface at the bottom of

510   an 8-well microscope glass-coverslip slide containing 200 µl 1% LB agarose per well

511   (Lab-Tek). Cells were then incubated for 75 min at 37 °C prior to imaging. In

512   filamentation experiments, 1 mL of cells grown overnight were sub-cultured into 4 mL of

513   LB containing 40 µg/ml of cefsulodin and incubated for 3 h at 37 °C. Cells were then

514   stained and mounted for microscopy using the above protocol. Cells were imaged using

515   an EVOS Fl-auto microscope in the McMaster Biophotonics Facility. Images were

516   acquired using a 60x oil immersion objective using a Texas Red filter, YFP filter, or

517   transmitted white light (no filter). Fiji (60) was used to adjust image brightness and

518   contrast, and to overlay brightfield and fluorescent images.

519

520   **Quantification of mCherry-PilO fluorescence**

521   Fluorescence was quantified using Fiji software (60). Each field in the Texas Red

522   (for mCherry) and YFP (for Fm1-43 Fx) filter sets were overlaid, and used with the

523   micrograph from the YFP filter for image analysis. A 250 µm^2 grid was added to each

524   field for precise documentation of the quantified cells. Moving systematically between

525   squares in the grid, cells that fulfilled the following criteria were selected: 1) not

526   contacting other cells; 2) normal rod morphology; and 3) a stable mCherry-PilO fusion

527   (diffuse cytoplasmic fluorescence implies cleavage of the tag in that cell). Cell lengths

528   and pixel intensities were measured from one cell pole to the other and normalized to 1

23

529   (i.e., each data point associated with length divided by the total length of the cell to yield

530   normalized 0 to 1 scale). Pixel intensity measurements in the YFP field (cell outline)

531   were then subtracted from the overlay field, producing mCherry-PilO pixel intensity

532   measurements alone in each cell on a scale from 0 to 1. From the data, an XY scatter

533   plot was generated to show the distribution of mCherry-PilO fluorescence over cell

534   length.

535

536   **ACKNOWLEDGEMENTS**

540

541   **REFERENCES**

542   1.   **Scheurwater EM, Burrows LL.** 2011. Maintaining network security: how

543   macromolecular structures cross the peptidoglycan layer. FEMS Microbiology

544   Letters **318:**1-9.

545   2.   **Mattick JS.** 2002. Type IV Pili and Twitching Motility. Annual Review of

546   Microbiology **56:**289-314.

547   3.   **Burrows LL.** 2012. *Pseudomonas aeruginosa* Twitching Motility: Type IV Pili in

548   Action. Annual Review of Microbiology **66:**493-520.

549   4.   **Siryaporn A, Kuchma SL, O'Toole GA, Gitai Z.** 2014. Surface attachment

550   induces *Pseudomonas aeruginosa* virulence. Proc Natl Acad Sci U S A

551   **111:**16860-16865.

552 5. **Heiniger RW, Winther-Larsen HC, Pickles RJ, Koomey M, Wolfgang MC.**

553   2010. Infection of human mucosal tissue by *Pseudomonas aeruginosa* requires

554   sequential and mutually dependent virulence factors and a novel pilus-associated

555   adhesin. Cellular Microbiology **12:**1158-1173.

556 6. **Golovkine G, Faudry E, Bouillot S, Elsen S, Attree I, Huber P.** 2016.

557   *Pseudomonas aeruginosa* Transmigrates at Epithelial Cell-Cell Junctions,

558   Exploiting Sites of Cell Division and Senescent Cell Extrusion. PLoS Pathog

559   **12:**e1005377.

560 7. **Chang YW, Rettberg LA, Treuner-Lange A, Iwasa J, Sogaard-Andersen L,**

561   **Jensen GJ.** 2016. Architecture of the type IVa pilus machine. Science

562   **351:**aad2001.

563 8. **Gold VA, Salzer R, Averhoff B, Kuhlbrandt W.** 2015. Structure of a type IV

564   pilus machinery in the open and closed state. Elife **4**.

565 9. **Koo J, Tang T, Harvey H, Tammam S, Sampaleanu L, Burrows LL, Howell**

566   **PL.** 2013. Functional Mapping of PilF and PilQ in the *Pseudomonas aeruginosa*

567   Type IV Pilus System. Biochemistry **52:**2914-2923.

568 10. **Koo J, Lamers RP, Rubinstein JL, Burrows LL, Howell PL.** 2016. Structure of

569   the *Pseudomonas aeruginosa* Type IVa Pilus Secretin at 7.4 A. Structure

570   **24:**1778-1787.

571 11. **Berry JL, Phelan MM, Collins RF, Adomavicius T, Tonjum T, Frye SA, Bird L,**

572   **Owens R, Ford RC, Lian LY, Derrick JP.** 2012. Structure and assembly of a

573   trans-periplasmic channel for type IV pili in *Neisseria meningitidis*. PLoS Pathog

574   **8:**e1002923.

575   12.   **Leighton TL, Buensuceso RNC, Howell PL, Burrows LL.** 2015. Biogenesis of

576   *Pseudomonas aeruginosa* type IV pili and regulation of their function.

577   Environmental Microbiology **17:**4148-4163.

578   13.   **Rocaboy M, Herman R, Sauvage E, Remaut H, Moonens K, Terrak M,**

579   **Charlier P, Kerff F.** 2013. The crystal structure of the cell division amidase AmiC

580   reveals the fold of the AMIN domain, a new peptidoglycan binding domain.

581   Molecular Microbiology **90:**267-277.

582   14.   **Ayers M, Sampaleanu LM, Tammam S, Koo J, Harvey H, Howell PL, Burrows**

583   **LL.** 2009. PilM/N/O/P Proteins Form an Inner Membrane Complex That Affects

584   the Stability of the *Pseudomonas aeruginosa* Type IV Pilus Secretin. J Mol Biol

585   **394:**128-142.

586   15.   **Leighton TL, Dayalani N, Sampaleanu LM, Howell PL, Burrows LL.** 2015.

587   Novel Role for PilNO in Type IV Pilus Retraction Revealed by Alignment

588   Subcomplex Mutations. J Bacteriol **197:**2229-2238.

589   16.   **Sampaleanu LM, Bonanno JB, Ayers M, Koo J, Tammam S, Burley SK, Almo**

590   **SC, Burrows LL, Howell PL.** 2009. Periplasmic Domains of *Pseudomonas*

591   *aeruginosa* PilN and PilO Form a Stable Heterodimeric Complex. J Mol Biol

592   **394:**143-159.

593   17.   **Tammam S, Sampaleanu LM, Koo J, Sundaram P, Ayers M, Chong AP,**

594   **Forman-Kay JD, Burrows LL, Howell PL.** 2011. Characterization of the PilN,

595   PilO and PilP type IVa pilus subcomplex. Molecular Microbiology **82:**1496-1514.

596   18.   **Karuppiah V, Derrick JP.** 2011. Structure of the PilM-PilN inner membrane type

597   IV pilus biogenesis complex from *Thermus thermophilus*. J Biol Chem

598   **286:**24434-24442.

599   19.   **McCallum M, Tammam S, Little DJ, Robinson H, Koo J, Shah M, Calmettes**

600   **C, Moraes TF, Burrows LL, Howell PL.** 2016. PilN binding modulates the

601   structure and binding partners of the *Pseudomonas aeruginosa* Type IVa Pilus

602   protein PilM. J Biol Chem **291:**11003-11015.

603   20.   **Tammam S, Sampaleanu LM, Koo J, Manoharan K, Daubaras M, Burrows**

604   **LL, Howell PL.** 2013. PilMNOPQ from the *Pseudomonas aeruginosa* type IV

605   pilus system form a transenvelope protein interaction network that interacts with

606   PilA. J Bacteriol **195:**2126-2135.

607   21.   **Leighton TL, Yong DH, Howell PL, Burrows LL.** 2016. Type IV Pilus Alignment

608   Subcomplex Components PilN and PilO Form Homo- and Heterodimers In Vivo.

609   J Biol Chem doi:10.1074/jbc.M116.738377.

610   22.   **Gotoh N, Nunomura K, Nishino T.** 1990. Resistance of *Pseudomonas*

611   *aeruginosa* to cefsulodin: modification of penicillin-binding protein 3 and mapping

612   of its chromosomal gene. J Antimicrob Chemo **25:**513-523.

613   23.   **Davis BM, Waldor MK.** 2013. Establishing polar identity in gram-negative rods.

614   Curr Opin Microbiol **16:**752-759.

615   24.   **Hu Z, Mukherjee A, Pichoff S, Lutkenhaus J.** 1999. The MinC component of

616   the division site selection system in *Escherichia coli* interacts with FtsZ to prevent

617   polymerization. PNAS **96:**14819-14824.

27

618   25.   **Burrows LL.** 2013. A new route for polar navigation. Molecular Microbiology

619   **90:**919-922.

620   26.   **Friedrich C, Bulyha I, Søgaard Andersen L.** 2014. Outside-in assembly

621   pathway of the type IV pilus system in *Myxococcus xanthus*. J Bacteriol **196:**378-

622   390.

623   27.   **Semmler ABT, Whitchurch CB, Leech AJ, Mattick JS.** 2000. Identification of a

624   novel gene, *fimV*, involved in twitching motility in *Pseudomonas aeruginosa*.

625   Microbiology **146:**1321-1332.

626   28.   **Wehbi H, Portillo E, Harvey H, Shimkoff AE, Scheurwater EM, Howell PL,**

627   **Burrows LL.** 2011. The peptidoglycan-binding protein FimV promotes assembly

628   of the *Pseudomonas aeruginosa* type IV pilus secretin. J Bacteriol **193:**540-550.

629   29.   **Cowles KN, Moser TS, Siryaporn A, Nyakudarika N, Dixon W, Turner JJ,**

630   **Gitai Z.** 2013. The putative Poc complex controls two distinct *Pseudomonas*

631   *aeruginosa* polar motility mechanisms. Molecular Microbiology **90:**923-938.

632   30.   **Huang B, Ru K, Yuan Z, Whitchurch CB, Mattick JS.** 2004. tonB3 is required

633   for normal twitching motility and extracellular assembly of type IV pili. J Bacteriol

634   **186:**4387-4389.

635   31.   **Bernhardt TG, De Boer PAJ.** 2003. The *Escherichia coli* amidase AmiC is a

636   periplasmic septal ring component exported via the twin-arginine transport

637   pathway. Molecular Microbiology **48:**1171-1182.

638   32.   **Heidrich C, Templin MF, Ursinus A, Merdanovic M, Berger J, Schwarz H, de**

639   **Pedro MA, Holtje J-V.** 2001. Involvement of N-acetylmuramyl-L-alanine

640   amidases in cell separation and antibiotic induced autolysis of *Escherichia coli*.

641   Molecular Microbiology **41:**167-178.

642 33. **Peters NT, Dinh T, Bernhardt TG.** 2011. A fail-safe mechanism in the septal ring

643   assembly pathway generated by the sequential recruitment of cell separation

644   amidases and their activators. J Bacteriol **193:**4973-4983.

645 34. **Buist G, Steen A, Kok J, Kuipers OP.** 2008. LysM, a widely distributed protein

646   motif for binding to (peptido)glycans. Molecular Microbiology **68:**838-847.

647 35. **Duncan TR, Yahashiri A, Arends SJR, Popham DL, Weiss DS.** 2013.

648   Identification of SPOR domain amino acids important for septal localization,

649   peptidoglycan binding, and a disulfide bond in the cell division protein FtsN. J

650   Bacteriology **195:**5308-5315.

651 36. **Mesnage Sep, Dellarole M, Baxter NJ, Rouget J-B, Dimitrov JD, Wang N,**

652   **Fujimoto Y, Hounslow AM, Lacroix-Desmazes Seb, Fukase K, Foster SJ,**

653   **Williamson MP.** 2014. Molecular basis for bacterial peptidoglycan recognition by

654   LysM domains. Nat Communications **5:**1-11.

655 37. **de Souza RF, Anantharaman V, de Souza SJ, Aravind L, Gueiros-Filho FJ.**

656   2008. AMIN domains have a predicted role in localization of diverse periplasmic

657   protein complexes. Bioinformatics **24:**2423-2426.

658 38. **Ramirez-Arcos S, Szeto J, Beveridge T, Victor C, Francis F, Dillon J.** 2001.

659   Deletion of the cell-division inhibitor MinC results in lysis of *Neisseria*

660   *gonorrhoeae*. Microbiology **147:**225-237.

661 39. **Buensuceso RNC, Nguyen Y, Zhang K, Daniel-Ivad M, Sugiman-Marangos**

662   **SN, Fleetwood AD, Zhulin IB, Junop MS, Howell PL, Burrows LL.** 2016. The

663   conserved TPR-containing C-terminal domain of *Pseudomonas aeruginosa* FimV

664   is required for its cAMP-dependent and independent functions. J Bacteriol

665   **198:**2263-2274.

666 40.   **Kirkpatrick CL, Viollier PH.** 2012. Cell polarity: ParA-logs gather around the

667   Hub. Curr Biol **22:**R1055-1057.

668 41.   **Rossmann F, Brenzinger S, Knauer C, Dorrich AK, Bubendorfer S, Ruppert**

669   **U, Bange G, Thormann KM.** 2015. The role of FlhF and HubP as polar landmark

670   proteins in *Shewanella putrefaciens* CN-32. Mol Microbiol **98:**727-742.

671 42.   **Takekawa N, Kwon S, Nishioka N, Kojima S, Homma M.** 2016. HubP, a polar

672   landmark protein, regulates flagellar number by assisting in the proper polar

673   localization of FlhG in *Vibrio alginolyticus*. J Bacteriol doi:10.1128/JB.00462-16.

674 43.   **Yamaichi Y, Bruckner R, Ringgaard S, Moll A, Cameron DE, Briegel A,**

675   **Jensen GJ, Davis BM, Waldor MK.** 2012. A multidomain hub anchors the

676   chromosome segregation and chemotactic machinery to the bacterial pole.

677   Genes Dev **26:**2348-2360.

678 44.   **Inclan YF, Persat A, Greninger A, Von Dollen J, Johnson J, Krogan N, Gitai**

679   **Z, Engel JN.** 2016. A scaffold protein connects type IV pili with the Chp

680   chemosensory system to mediate activation of virulence signaling in

681   *Pseudomonas aeruginosa*. Mol Microbiol **101:**590-605.

682 45.   **Korotkov KV, Pardon E, Steyaert J, Hol WG.** 2009. Crystal structure of the N-

683   terminal domain of the secretin GspD from ETEC determined with the assistance

684   of a nanobody. Structure **17:**255-265.

685 46. **Nudleman E, Wall D, Kaiser D.** 2005. Cell-to-cell Transfer of Bacterial Outer

686   Membrane Lipoproteins. Science **309:**125-127.

687 47. **Typas A, Banzhaf M, van den Berg van Saparoea B, Verheul J, Biboy J,**

688   **Nichols RJ, Zietek M, Beilharz K, Kannenberg K, von Rechenberg M,**

689   **Breukink E, den Blaauwen T, Gross CA, Vollmer W.** 2010. Regulation of

690   peptidoglycan synthesis by outer-membrane proteins. Cell **143:**1097-1109.

691 48. **Jean NL, Bougault CM, Lodge A, Derouaux A, Callens G, Egan AJ, Ayala I,**

692   **Lewis RJ, Vollmer W, Simorre JP.** 2014. Elongated structure of the outer-

693   membrane activator of peptidoglycan synthesis LpoA: implications for PBP1A

694   stimulation. Structure **22:**1047-1054.

695 49. **Nandi S, Swanson S, Tomberg J, Nicholas RA.** 2015. Diffusion of antibiotics

696   through the PilQ secretin in *Neisseria gonorrhoeae* occurs through the immature,

697   sodium dodecyl sulfate-labile form. J Bacteriol **197:**1308-1321.

698 50. **Demchick P, Koch AL.** 1996. The Permeability of the Wall Fabric of *Escherchia*

699   *coli* and *Bacillus subtilis*. J Bacteriol **178:**768-773.

700 51. **Wang P, Robert L, Pelletier J, Dang WL, Taddei F, Wright A, Jun S.** 2010.

701   Robust growth of *Escherichia coli*. Curr Biol **20:**1099-1103.

702 52. **Korotkov KV, Johnson TL, Jobling MG, Pruneda J, Pardon E, Heroux A,**

703   **Turley S, Steyaert J, Holmes RK, Sandkvist M, Hol WG.** 2011. Structural and

704   functional studies on the interaction of GspC and GspD in the type II secretion

705   system. PLoS Pathog **7:**e1002228.

706 53. **Wang X, Pineau C, Gu S, Guschinskaya N, Pickersgill RW, Shevchik VE.**

707   2012. Cysteine scanning mutagenesis and disulfide mapping analysis of

708   arrangement of GspC and GspD protomers within the type 2 secretion system. J

709   Biol Chem **287:**19082-19093.

710   54.   **Lamers RP, Nguyen UT, Nguyen Y, Buensuceso RN, Burrows LL.** 2015. Loss

711   of membrane-bound lytic transglycosylases increases outer membrane

712   permeability and beta-lactam sensitivity in *Pseudomonas aeruginosa*.

713   Microbiologyopen **4:**879-895.

714   55.   **Hoang TT, Karkhoff-Schweizer RR, Kutchma AJ, Schweizer HP.** 1998. A

715   broad-host-range Flp-FRT recombination system for site-specific excision of

716   chromosomally-located DNA sequences: application for isolation of unmarked

717   *Pseudomonas aeruginosa* mutants. Gene **212:**77-86.

718   56.   **Shu X, Shaner NC, Yarbrough CA, Tsien RY, Remington SJ.** 2006. Novel

719   Chromophores and Buried Charges Control Color in mFruits. Biochemistry

720   **45:**9639-9647.

721   57.   **Lieberman JA, Petro CD, Thomas S, Yang A, Donnenberg MS.** 2015. Type IV

722   pilus secretins have extracellular C termini. MBio **6:**e00322-15.

723   58.   **Asikyan ML, Kus JV, Burrows LL.** 2008. Novel proteins that modulate type IV

724   pilus retraction dynamics in *Pseudomonas aeruginosa*. Journal of Bacteriology

725   **190:**7022-7034.

726   59.   **Kus JV, Tullis E, Cvitkovitch DG, Burrows LL.** 2004. Significant differences in

727   type IV pilin allele distribution among *Pseudomonas aeruginosa* isolates from

728   cystic fibrosis (CF) versus non-CF patients. Microbiology **150:**1315-1326.

729   60.   **Schindelin J, Arganda-Carreras I, Frise E, Kaynig V, Longair M, Pietzsch T,**

730   **Preibisch S, Rueden C, Saalfeld S, Schmid B, Tinevez J-Y, White DJ,**

731   **Hartenstein V, Eliceiri K, Tomancak P, Cardona A.** 2012. Fiji: an open-source

732   platform for biological-image analysis. Nature Methods **9:**676-682.

733 61. **Simon R, Priefer U, Puhler A.** 1983. A Broad Host Range Mobilization System

734   for in vivo Genetic Engineering: Transposon Mutagenesis in Gram Negative

735   Bacteria. Nature Biotechnology **1:**784-791.

736 62. **Takhar HK, Kemp K, Kim M, Howell PL, Burrows LL.** 2013. The platform

737   protein is essential for type IV pilus biogenesis. J Biol Chem **288:**9721-9728.

738 63. **Kus JV, Kelly J, Tessier L, Harvey H, Cvitkovitch DG, Burrows LL.** 2008.

739   Modification of *Pseudomonas aeruginosa* Pa5196 Type IV Pilins at Multiple Sites

740   with D-Araf by a Novel GT-C Family Arabinosyltransferase, TfpW. Journal of

741   Bacteriology **190:**7464-7478.

742 64. **Nguyen Y, Harvey H, Sugiman-Marangos S, Bell SD, Buensuceso RNC,**

743   **Junop MS, Burrows LL.** 2015. Structural and Functional Studies of the

744   *Pseudomonas aeruginosa* Minor Pilin, PilE. Journal of Biological Chemistry

745   **290:**26856-26865.

746

747

748

749

750

751

752

753

33

754 **TABLES**

755 **Table 1. Bacterial strains and plasmids**

Strain	Description	Source
E. coli		
DH5α	F-, φ80lacZ, M15, Δ(_lacZYA-argF_), U169, _recA1, endA1, hsdR17(rk-,mk+), phoAsupE44, thi-1, gyrA96, relA1_, λ-	Invitrogen
SM10	_thi-1, thr, leu, tonA, lacy, supE, recA_, RP4-2-Tcr::Mu, Kmr; mobilizes plasmids into _P. aeruginosa_ via conjugation	(61)
P. aeruginosa		
PAK	Wild type	J. Boyd
ΔpilM	Deletion of _pilM_	(62)
pilP::FRT	FRT scar at nucleotide 86 of _pilP_	(14)

pilQ::FRT	FRT scar at nucleotide 571 of *pilQ*	(9)
pilA::FRT	FRT scar at SphI site within *pilA*	(63)
ΔpilF	*pilF* deletion strain	This study
ΔminC	*minC* deletion strain	This study
mCherry-PilO	In frame fusion of *mCherry* to the 5' end of *pilO* on the PAK chromosome	This study
ΔpocA	*pocA* deletion strain	(29)
ΔfimV	*fimV* deletion strain	(39)
fimVΔLysM	*fimV* with in frame deletion of LysM domain	(28)
mCherry-PilO *ΔpilM*	deletion of *pilM* in mCherry-PilO strain	This study
mCherry-PilO *pilP*::FRT	FRT scar in *pilP* at nucleotide 86 in mCherry-PilO strain	This study
mCherry-PilO *pilQ*::FRT	FRT scar at position 571 within *pilQ* in mCherry-PilO strain	This study
mCherry-PilO *ΔpilF*	deletion of *pilF* in	This study

	mCherry-PilO strain	
mCherry-PilO *ΔminC*	deletion of *minC* in mCherry-PilO strain	This study
mCherry-PilO *ΔpocA*	deletion of *pocA* in mCherry-PilO background	This study
mCherry-PilO *ΔfimV*	deletion of *fimV* in mCherry-PilO background	This study
mCherry-PilO *fimVΔLysM*	Insertion of *mCherry* at the 5' end of *pilO* with *fimV* containing deletion of LysM domain	This study
Plasmids	**Description**	**Source**
pEX18Gm	Suicide vector used for gene replacement, Gm	(55)
pEX18Ap	Suicide vector used for gene replacement, Ap	(55)
pBADGr	Arabinose inducible protein expression vector	(58)
pFLP2	Suicide vector containing	(55)

36

	Flp recombinase	
pEX18Gm::*mCherry-pilO*	Suicide vector containing *mCherry-pilO*, subcloned from pUC57 (Genscript) using EcoRI/HindIII	This study
pEX18Gm::*ΔpilF*	Suicide vector containing *pilF* deletion, cloned using BamHI/HindIII	This study
pEX18Gm::*ΔminC*	Suicide vector containing *minC* deletion, cloned using BamHI/HindIII	This study
pEX18Gm::*ΔpocA*	Suicide vector containing *pocA* deletion, cloned using EcoRI/XbaI	This study
pEX18Ap-*pilQ*::GmFRT	Suicide vector containing PAK *pilQ* disrupted with FRT-flanked Gm cassette at position 571	This study
pBADGr::*pilQ-mCherry*	*pilQ-mCherry* complementation construct, cloned using EcoRI/HindIII	This study
pBADGr::*pilF*	*pilF* complementation	This study

37

	construct, cloned using SphI/HindIII	
pBADGr::*pilQ*	*pilQ* complementation construct, cloned using EcoRI/HindIII	This study
pBADGr::*pilQΔAMIN*	*pilQΔAMIN* complementation construct, cloned using EcoRI/HindIII	This study
pBADGr::*pocA*	*pocA* complementation construct, cloned using EcoRI/HindIII	This study
pBADGr::*fimV-yfp*	*fimV-yfp* complementation construct, cloned using KpnI/XbaI	This study

756

757

758

759 **Table 2. Primer sequences**

Name	Oligonucleotide sequence
PilF-Fwd	5'ACGCCTTGCAAGATCAACCTGATTCCG3'
PilF-Rev	5'TCGAACGCGCCGTTTTCCAGCTGACGC3'
PilF mid-Rev	5'GGCCGGTTTCTTCATTTGCAGCG3'
PilF Clone-Fwd	5'TCATGCATGCATGACTGTACGCGCCGCGCTGG3'
PilF Clone-Rev	5'TCATAAGCTTTCATTTTTCCGCCTGGAATTCCTG3'
MinC Fwd	5'GGATACGGCAACTGCACCACCAGCCAG3'
MinC Rev	5'GACGACGTTGACGAAGTCGTACACCAC3'
MinC mid-Rev	5'CGTGGCGGCGACAGACCTCGAGGA3'
PilN 3'-Fwd	5'GCCAACGTGTTCCAACTG3'
PilO Rev	5'CCACGCTGATCTGGATCG3'
PocA Fwd	5'GAATTCGGGGATATGCCACGTGTGGGA3'
PocA Rev	5'AAGCTTTGCGGCGGAATTTCACGCTTTGC3'
PocA Mid-Rev	5'GAGGATCTCTCCCAGCGG3'
PocA Clone-Fwd	5'TCATGAATTCGTGTGGGAACTGGTTCAAGCCGG3'

PocA Clone-Rev	5'TCATAAGCTTTCACGCTTTGCCTTCCTCGACGTAG3'
PilQ Clone-Fwd	5'AGAATTCCAACAGCAGTCTGTACAA3'
PilQ Clone-Rev	5'TCATAAGCTTTCAGCGACCGATTGCGATGGCCTG3'
PilQ 910-Fwd	5'CGACCTGAATCTGGTGGC3'
PilQ FRT-Chk Fwd	5'TTGATCATCAACCTGACCGCGCTGTCG3'
PilQ FRT-Chk Rev	5'TCATCGGCTTGATGCTGACGGTCAGG3'
pBAD mcs-Fwd	5'AAGTGTCTATAATCACGGCAGA3'
pBAD mcs-Rev	5'TCACTTCTGAGTTCGGCATGG3'
mCherry Rev	5'TCATGCATGCGCTTCCGCCGCTCTTGTACAGCTCGTC CATGCCGC3'
PilQ 5' Rev	5'TCATTCTAGAGTCCGCGGCGAGCAATGCCGGCGC3'
PilQ N0 Fwd	5'TCATTCTAGAGGCGAGAAACTGTCGCTGAACTTC3'
FimV Clone Fwd	5'GCGGGTACCATGGTTCGGCTTCG3'
FimV Clone Rev	5'GCGTCTAGAGGCCAGGCGCTCCA3'

760

761

762　**FIGURE LEGENDS**

763　**Figure 1. mCherry-PilO localizes to cell poles and future sites of cell division in _P._**

764　**_aeruginosa_**. **A**. Map of the T4aP alignment subcomplex operon showing _mCherry-pilO_

765　integration. **B**. The mCherry-PilO fusion was stable (~48 kDa product recognized by

766　both anti-PilO and anti-mCherry antibodies; a plasmid-encoded PilE-mCherry fusion –

767　open triangle – was used as a positive control for the latter; (64)) and functional for

768　twitching motility. **C**. mCherry-PilO localized to the poles of wild type cells and to the

769　septum in late-stage dividing cells. **D**. When cells were filamented using 40 µg/ml

770　cefsulodin, mCherry-PilO localized to the poles and at regularly spaced foci

771　(arrowheads). Scale bar = 3 µm. **E**. mCherry pixel intensity in 50 untreated cells after

772　normalization of length to 1 as described in the Methods.

773

774　**Figure 2. mCherry-PilO localizes to aberrantly localized septa in a _minC_ mutant.**

775　**A.** Transmission electron micrograph of a _minC_ mutant of _P. aeruginosa_ strain PAK. In

776　the absence of _minC_, cells have aberrantly located division sites (red arrows). Scale bar

777　= 1 µm. **B.** mCherry-PilO polar foci are indicated with white arrowheads while foci

778　localized to aberrantly placed septa are indicated with yellow arrows.

779

780　**Figure 3. Polar localization of T4aP alignment subcomplex requires PilQ.** In the

781　absence of PilM, mCherry-PilO is localized to **A.** poles and septa in untreated cells, and

782　**B.** poles and regularly spaced foci in cells treated with cefsulodin. In the absence of

783　PilQ, mCherry-PilO is delocalized in both **C.** untreated and **D.** antibiotic-filamented cells.

784　Similarly, in the absence of PilP, mCherry-PilO is delocalized in **E.** untreated and **F.**

41

785   antibiotic-treated cells**.** The last 3 panels show quantification of mCherry pixel intensity

786   in the absence of **G.** *pilM*, **H.** *pilQ*, or **I.** *pilP*, in 50 untreated cells after normalization of

787   length to 1 as described in the Methods. Scale bar = 3 μm.

788

789   **Figure 4. The AMIN domains of PilQ are required for polar localization of mCherry-**

790   **PilO. A.** Domain map of PilQ showing its PG-binding AMIN domains in blue.

791   Complementation of a *pilQ* rmutant expressing mCherry-PilO with full length *pilQ* re-

792   established its polar and septal localization (white arrowheads) in **B.** untreated cells, and

793   **C.** localization to the poles and regularly spaced foci in cefsulodin treated cells. When

794   the same mutant was complemented with a truncated version of *pilQ* that encodes only

795   N0-N1 and the secretin domains, mCherry-PilO was delocalized in both **D.** untreated

796   and **E.** antibiotic-treated cells. The last 3 panels show quantification of mCherry pixel

797   intensity in the presence of **F.** PilQ or **G.** PilQ lacking its AMIN domains, in 50 untreated

798   cells after normalization of length to 1 as described in the Methods. Scale bar = 3 μm.

799

800   **Figure 5. mCherry-PilO is polarly localized in the absence of *pilF*. A.** mCherry-PilO

801   localized to the poles and septa of late-stage dividing cells, marked by white

802   arrowheads. **B.** When cells were filamented with cefsulodin, mCherry-PilO localized to

803   the poles and to foci (arrows). Scale bar = 3 μm. Panel **C.** shows quantification of

804   mCherry pixel intensity in the *pilF* background, in 50 untreated cells after normalization

805   of length to 1 as described in the Methods.

806

807   **Figure 6. FimV is required for polar localization of mCherry-PilO.** In the absence of

808   FimV, mCherry-PilO was delocalized in **A.** untreated cells and **B.** cells treated with

809   cefsulodin. In cells expressing a version of FimV with an in-frame deletion of its PG-

810   binding domain (LysM), mCherry-PilO was delocalized in **C.** untreated and **D.** antibiotic-

811   treated cells. The last two panels show quantification of mCherry pixel intensity **F.** in the

812   absence of FimV or **G.** in the strain expressing FimV$_{\Delta LysM}$, in 50 untreated cells after

813   normalization of length to 1 as described in the Methods. Scale Bar = 3 µm.

814

815   **Figure 7. mCherry-PilO is delocalized in a *pocA* mutant.** In the absence of the polar

816   organelle coordinating protein, PocA, mCherry-PilO was delocalized in **A.** untreated

817   cells and **B.** cells treated with cefsulodin. When *pocA* was reintroduced *in trans*,

818   mCherry-PilO localization to the poles and septum was recovered (white arrowheads) in

819   **C.** untreated cells, as well as to **D.** the poles and regularly spaced foci in antibiotic-

820   treated cells. The last two panels show quantification of mCherry pixel intensity **E.** in the

821   absence of PocA and **F.** in the *pocA*-complemented mutant, in 50 untreated cells after

822   normalization of length to 1 as described in the Methods. Scale bar = 3 µm.

823

824   **Figure 8. FimV remains polarly localized in the absence of PocA. A**. FimV-YFP

825   remained localized to the cell poles (arrowheads) in a *pocA* mutant. **B.** FimV-YFP

826   localized to the poles in cefsulodin treated cells. Scale bar = 3 µm.
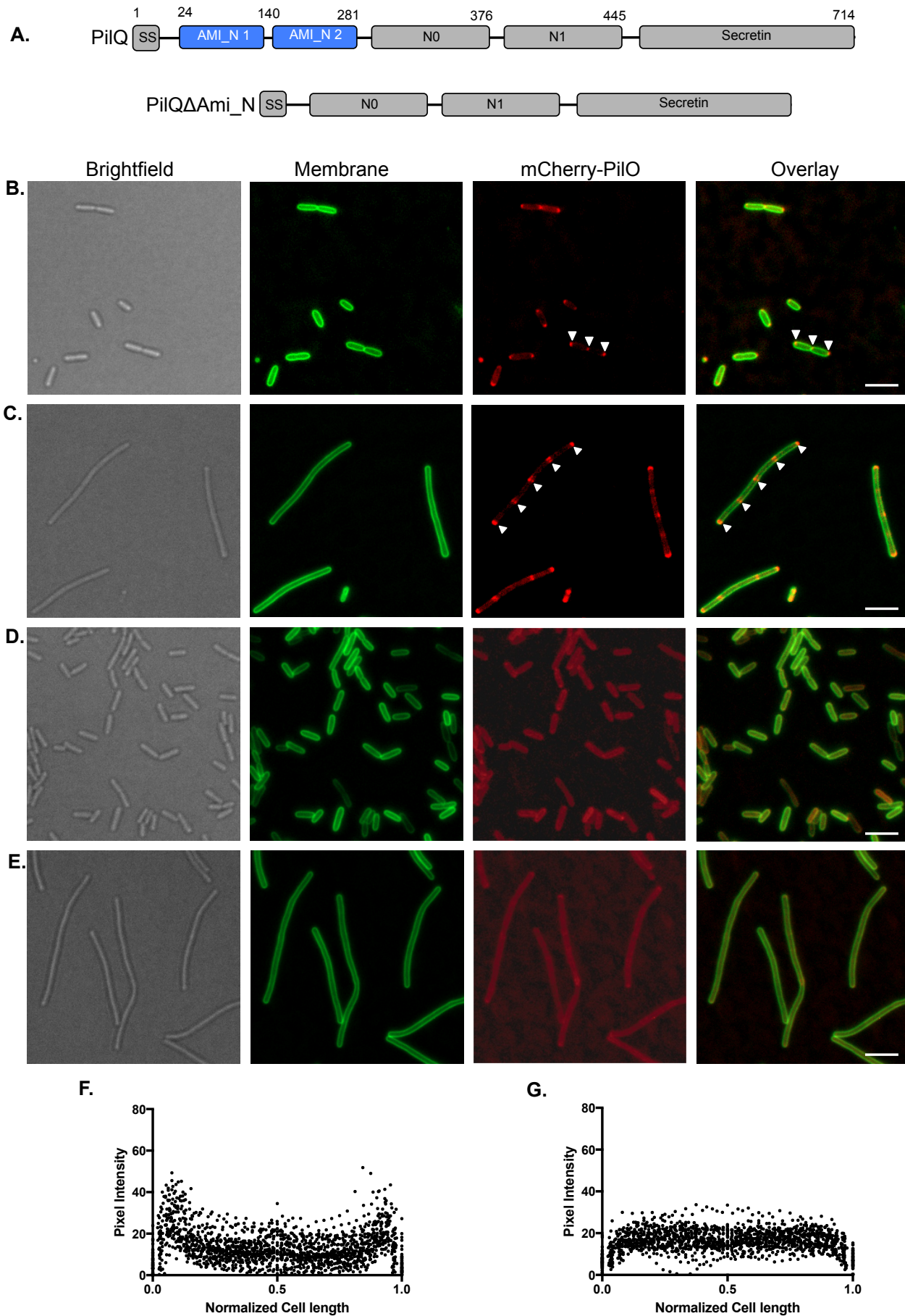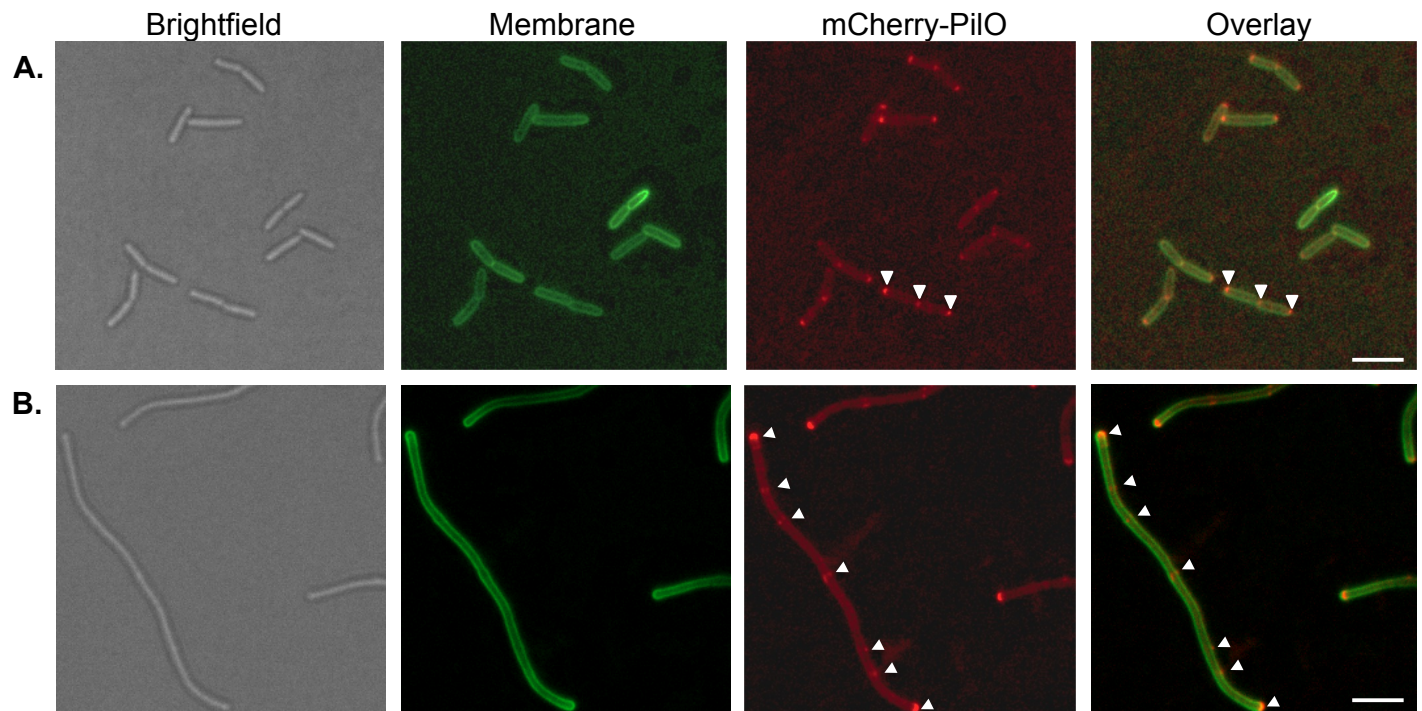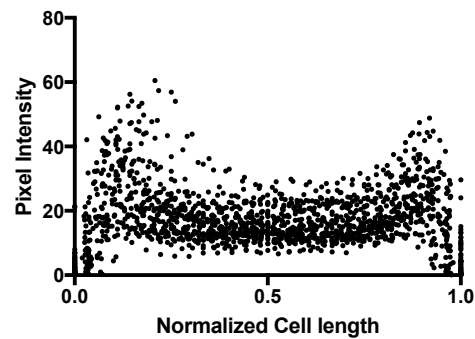
827

828

Carter et al. Figure 1
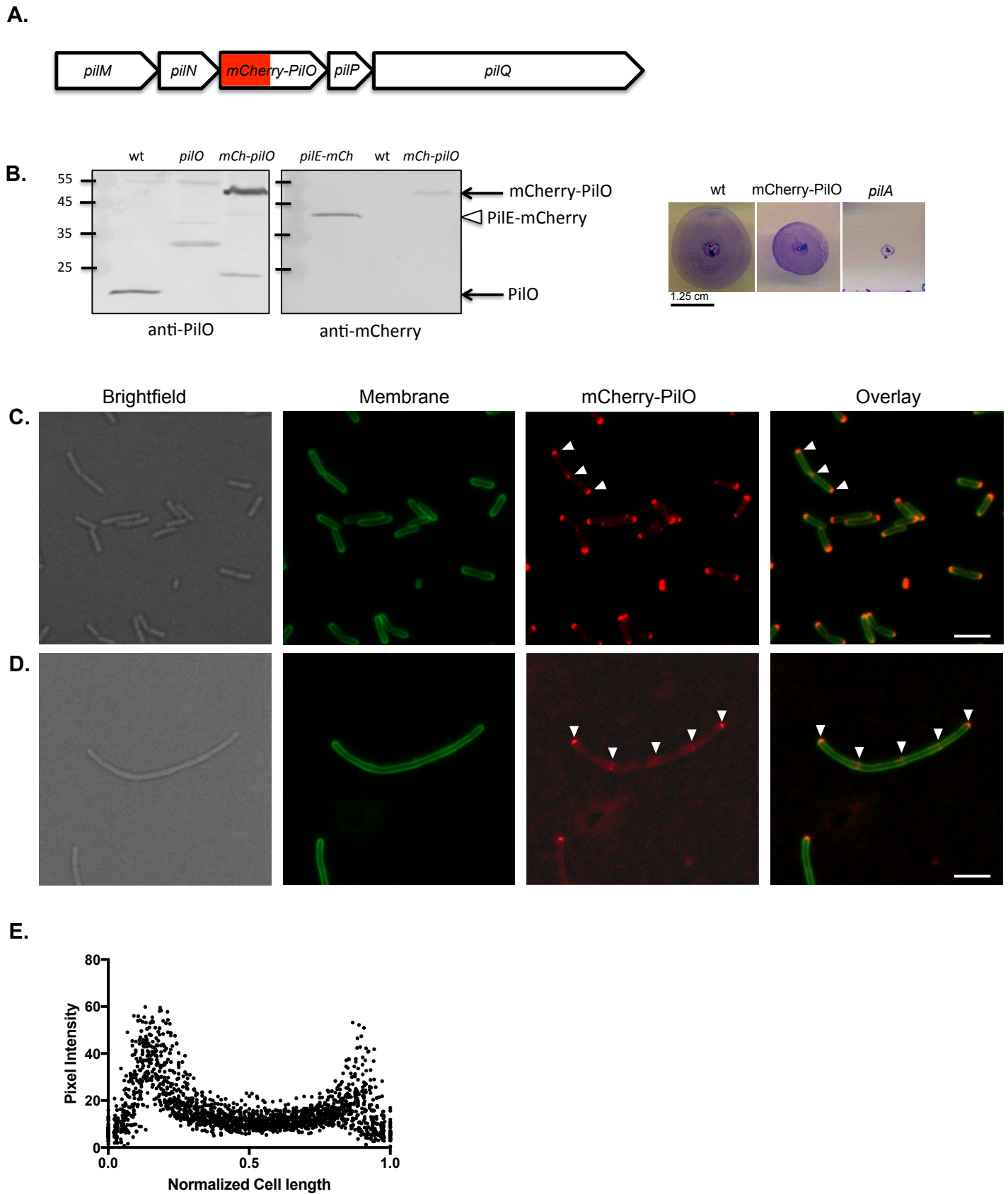
Carter et al. Figure 2
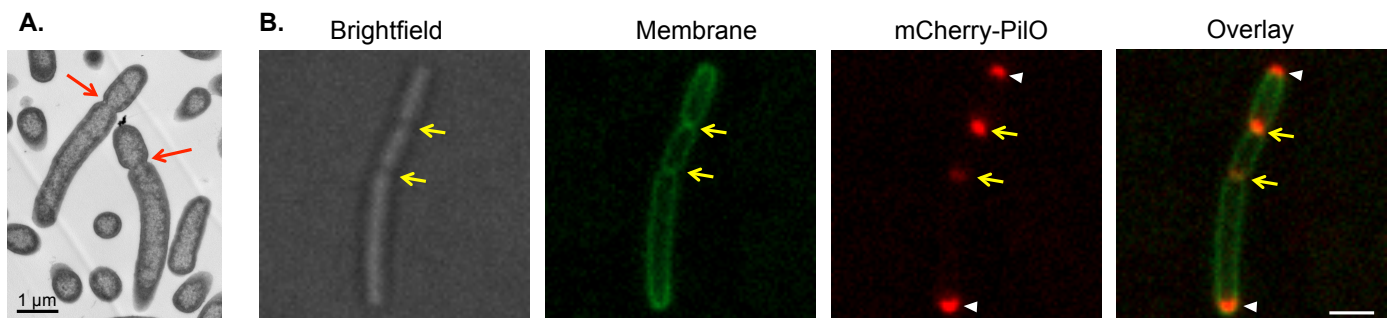
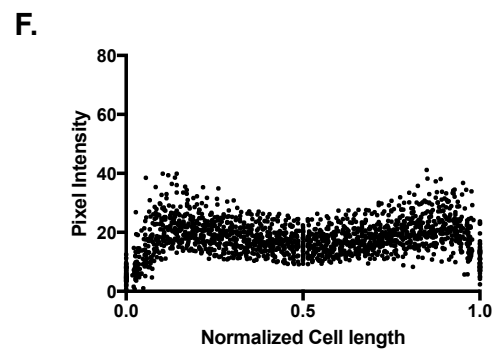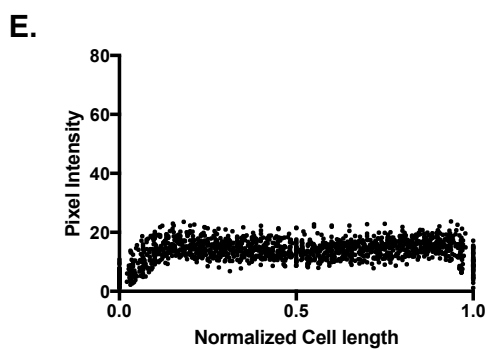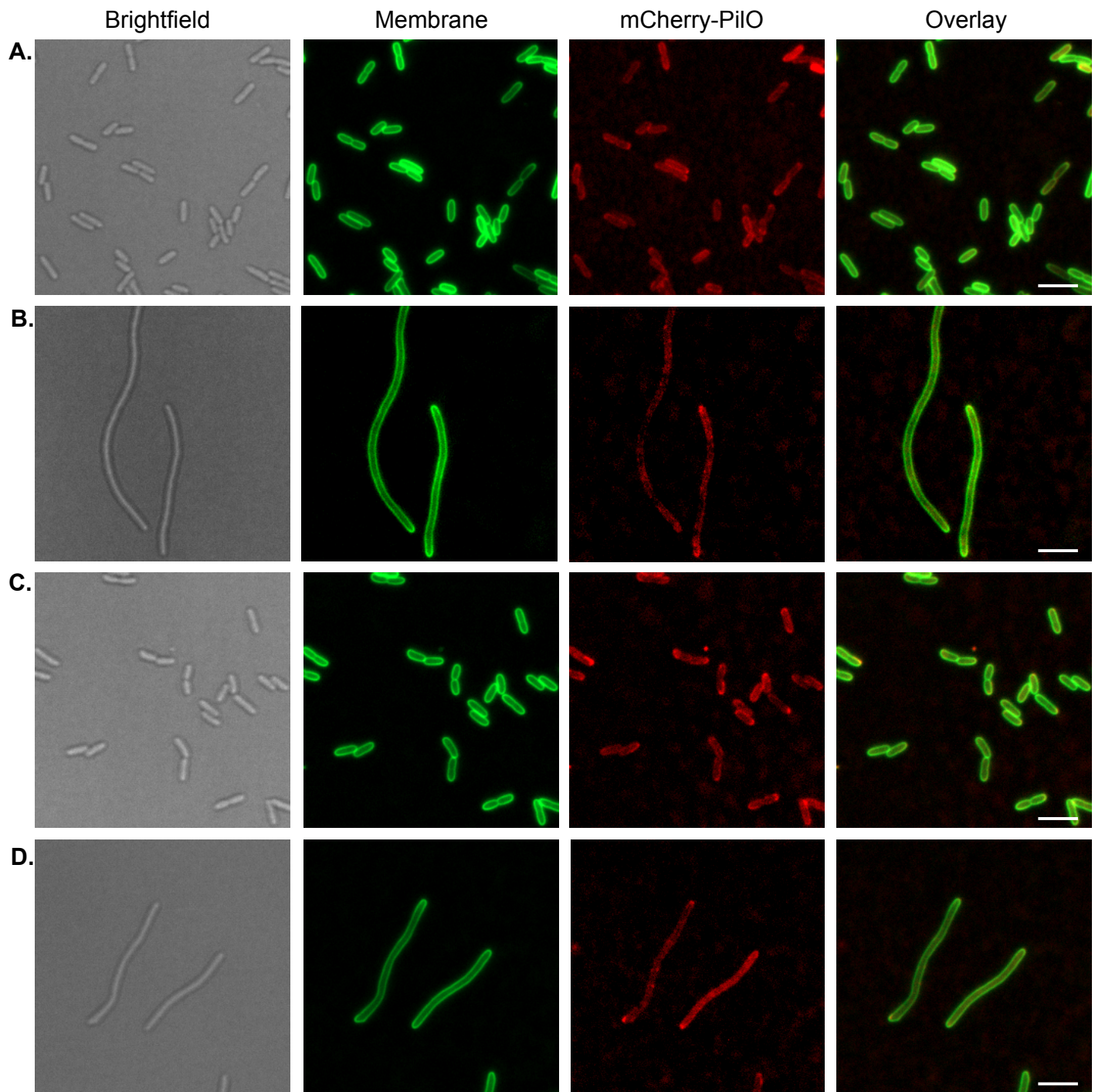# Carter et al. Figure 3
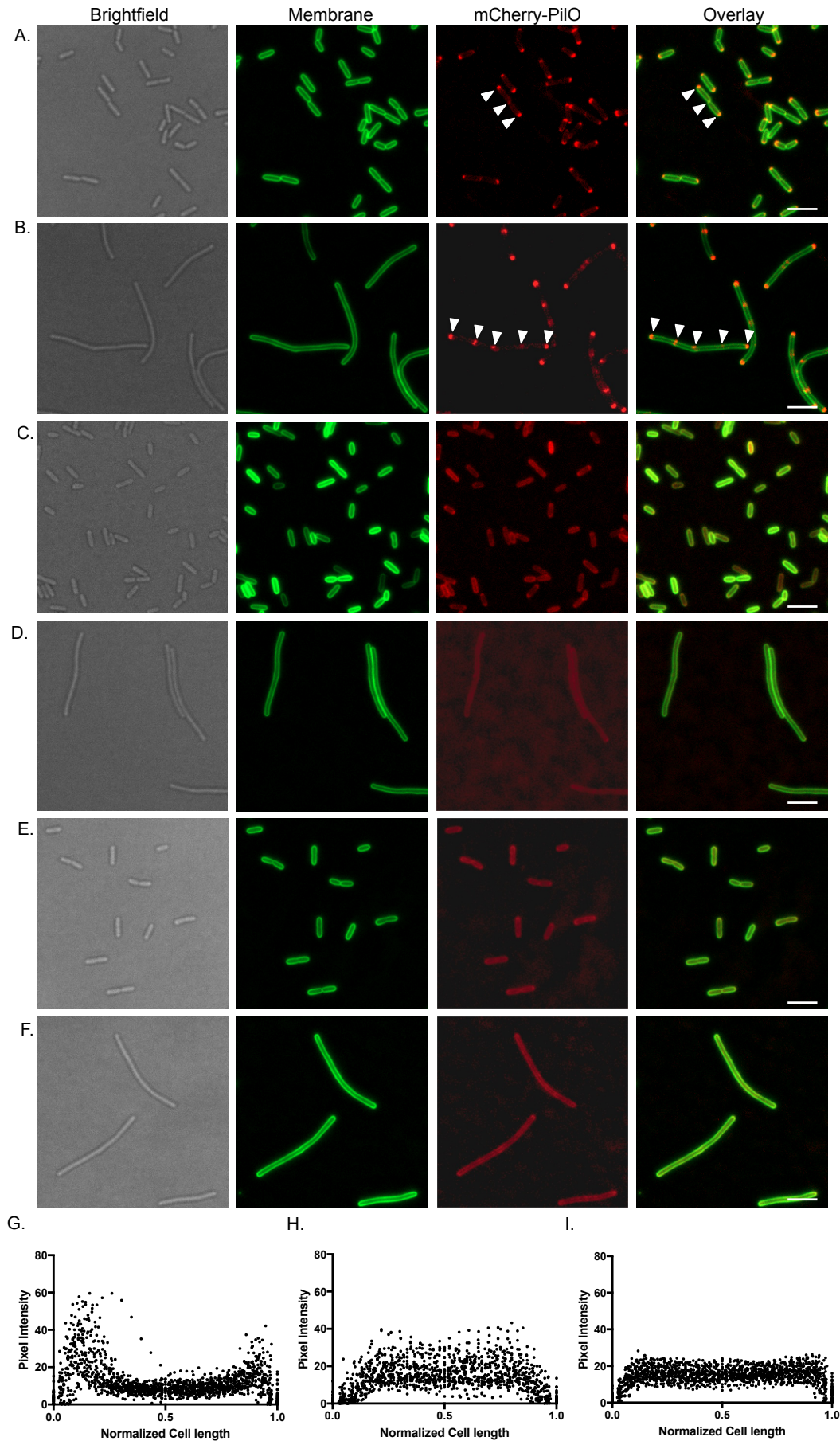
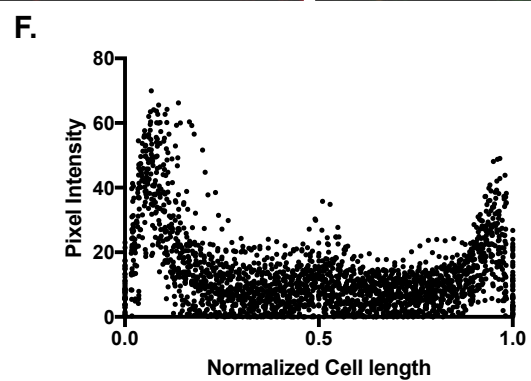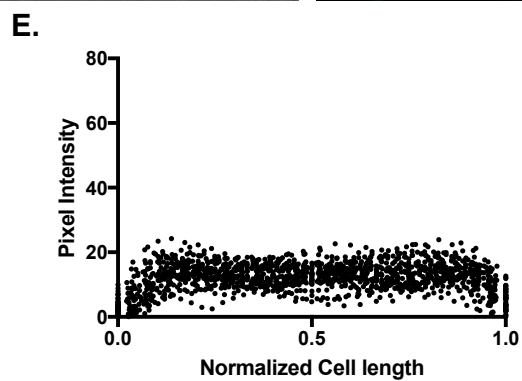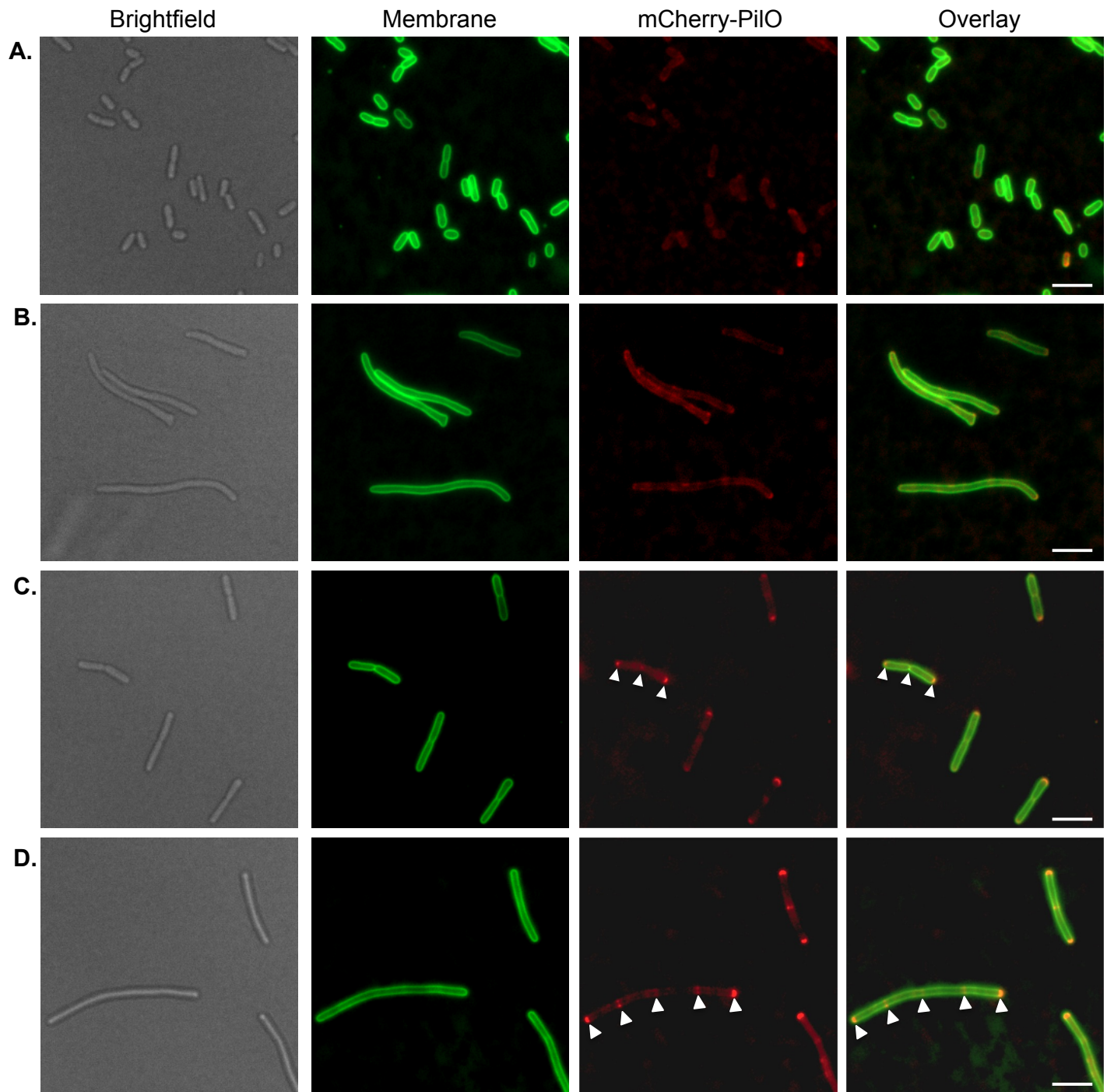# Carter et al. Figure 4

Carter et al. Figure 5

Carter et al. Figure 6

Carter et al. Figure 7

Carter et al. Figure 8